ELSEVIER

Journal of Nuclear Materials 307–311 (2002) 106–110

journal of nuclear materials

www.elsevier.com/locate/jnucmat

Melt layer behavior of metal targets irradiatead by powerful plasma streams

A.N. Bandura [a], O.V. Byrka [a], V.V. Chebotarev [a], I.E. Garkusha [a,*], V.A. Makhlaj [a], D.G. Solyakov [a], V.I. Tereshin [a], H. Wuerz [b]

[a] *Institute of Plasma Physics, NSC KIPT, Kharkov 61108, Ukraine*
[b] *Forschungszentrum Karlsruhe, IHM, 76021 Karlsruhe, Germany*

Abstract

In this paper melt layer erosion of metal targets under pulsed high-heat loads is studied. Experiments with steel, copper, aluminum and titanium samples were carried out in two plasma accelerator devices with different time durations of the heat load. The surfaces of the resolidified melt layers show a considerable roughness with microcraters and ridge like relief on the surface. For each material the mass loss was determined. Melt layer erosion by melt motion was clearly identified. However it is masked by boiling, bubble expansion and bubble collapse and by formation of a Kelvin–Helmholtz instability. The experimental results can be used for validation of numerical codes which model melt layer erosion of metallic armour materials in off-normal events, in tokamaks.
© 2002 Elsevier Science B.V. All rights reserved.

1. Introduction

The lifetime of the divertor and first wall armour against high-heat loads during off-normal events and ELMS is of concern in the design of a tokamak fusion reactor. It was shown in numerical simulations of ITER-FEAT off-normal events [1] that melt layer motion produces significant macroscopic erosion of metals. This process is considered as the most important one from the point of view of the lifetime of metallic armours [1–3]. The first results of a detailed numerical analysis of melt layer erosion are presented at this conference [4,5]. For validation of the numerical models, additional experimental data on melt layer erosion under pulsed high-heat loads are needed. As a first step in such experiments, it is convenient to use pure materials, such as Al, Cu, Ti, with well known thermophysial properties (tungsten will be used in further experiments). This paper presents experimental results of melt layer erosion and metals behavior under irradiation with high-power plasma streams generated in two different plasma accelerators with different heat load levels and different time duration. The experiments can simulate the magnitude of the tokamak off-normal heat loads but not the time duration of such events. In a tokamak the time duration of the off-normal heat loads might be up to orders of magnitudes larger, and the guiding magnetic field also is considerably larger.

2. Experimental devices

Experiments with steel, aluminum, copper and titanium samples were carried out in two plasma accelerator devices: the pulsed plasma accelerator (PPA) and the quasi-stationary plasma accelerator (QSPA). The facilities are described in detail in [6,7]. The PPA generates plasma streams with average diameter of 8 cm, ion energies up to 2 keV, ion density $\sim 2 \times 10^{14}$ cm^{-3}, maximum specific power up to 100 GW/m^2 and duration of the heat load of 5–10 μs.

Melt layer dynamics and erosion under longer pulse durations were investigated in the QSPA facility with

* Corresponding author. Tel.: +380-572 356 305/726; fax: +380-572 352 664.
E-mail address: garkusha@ipp.kharkov.ua (I.E. Garkusha).

0022-3115/02/$ - see front matter © 2002 Elsevier Science B.V. All rights reserved.
PII: S0022-3115(02)00995-9

hydrogen plasma streams with time duration up to 130–140 μs, average density of 4×10^{16} cm^{-3}, heat loads up to 200 GW/m^2 and ion energy up to 0.6 keV. A guiding magnetic field of 0.54 T was applied in these experiments. The diameter of the QSPA plasma stream achieved 10–12 cm.

A number of diagnostics were used in the present experiments, namely: the plasma stream velocity was measured by the flight time of the plasma stream between two magnetic probes, the electron density in the plasma stream was measured by Stark broadening of the H_β spectral line, the power density was calculated on the basis of measurements of the time dependencies of the plasma stream density and its velocity, radial distributions of the plasma stream energy density were measured using a movable copper calorimeter [7].

In the experiments the target surface was perpendicular to the impacting plasma stream. Two kinds of samples were used in the experiments. The composite samples consist of a central disk of diameter of 50 and 7 mm in thickness, which was inserted in a ring of the same thickness of diameters of 53 and 120 mm. Such samples were used for mass-loss measurements. This geometry provided both homogeneity of the plasma energy density within the disk and accuracy of weight measurements. For analysis of the melt surface, samples with a diameter of 120 mm and thickness of 30–40 mm (to avoid sample bending) were used. To protect the sample edges from plasma exposure, the outer part of the sample was covered by a molybdenum screen of diameter of 120 mm having a rectangular hole of 45×100 mm^2 for plasma exposure. The unexposed part of the sample was used as a reference for profilometry. The distance between the screen (1 mm in thickness) and the sample surface was 1.5 mm.

An optical microscope was used for surface analysis. A profilometer with an accuracy of 0.4 μm was used for analysis of the surface structure of the melt layer. The weight loss was measured with balance with an accuracy of ±2 mg.

3. Results of experiments

3.1. Structure of the melt surface

The profile across the edge region of an aluminum sample is presented in Fig. 1 for one QSPA exposure. Three regions can be easily seen: a non-melted region at the right side of the profile, the region where melting begins below an oxide film and the region of strong melting with considerable surface roughness (left side).

A hill with a height of about 40 μm and a length of about 1 mm is clearly seen at the right side just under the protective stripe. This is a clear indication of melt layer motion, which shifts the melted material to the sample periphery. A considerable roughness is observed at the melted region. It is difficult to determine an erosion crater because of the large roughness of the surface with heights up to 300 μm. The large roughness also masks the melt motion to the peripheral part of the sample. With an increasing number of exposures, the surface roughness increased upto 1 mm.

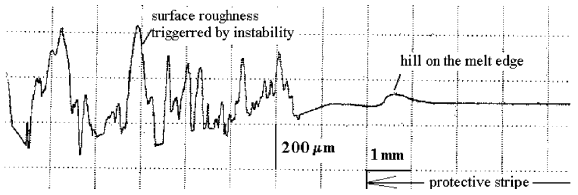

Fig. 1. The profile at the edge region of an aluminum target with protective stripes at the target edge.

The edge of the melted zone of a Cu sample is shown in Fig. 2(a) after one QSPA pulse. Droplets with sizes up

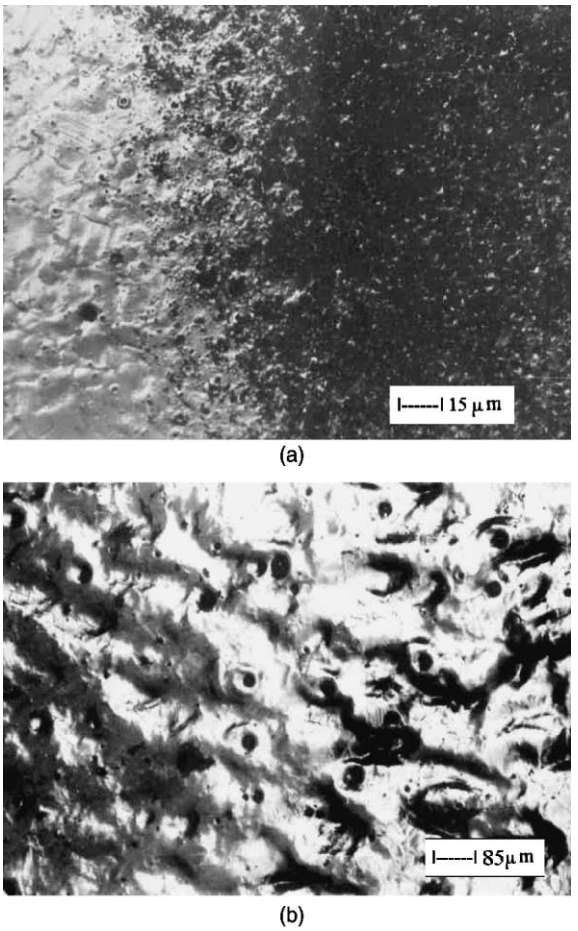

Fig. 2. Surface of copper after QSPA irradiation: (a) edge of melt zone after irradiation with 1 shot and (b) melt region after irradiation with 15 shots.

to a few microns splashed from the melt, and small regions of melting are observed outside of the melt region. After irradiation with 15 pulses a wave-like structure appears on the resolidified surface (Fig. 2(b)). The distance between local peaks is about 100–140 μm. Pores with sizes up to 30 μm in diameter indicate boiling, bubble levitation and bubble collapse. Droplets of sizes up to 100–200 μm are observed outside of the melt region. The droplet velocity was evaluated on the base of the droplet size, the distance of their displacement and the duration of the incident plasma stream exposure. The estimated velocity of the droplets depends on their size but is typically more than 5×10^2 cm/s. From the obtained results it is concluded that volumetric boiling with bubble formation, bubble collapse and splashing of melted material occurs. Additionally, the wavy structure indicates evolution of a Kelvin–Helmholtz instability [1] triggered by the plasma flowing along the melt surface.

According to XRD data the phase content in the copper melt layer after plasma irradiation and resolidification is identical to the initial sample. A decrease in the lattice parameter of copper and a smaller width of the diffraction pattern was registered by X-ray diffraction analysis. These results are similar to the data obtained earlier for tungsten irradiation [8]. One of the possible explanations for the decreased lattice parameter in the resolidified layer could be a compression stress arising under high-speed melting and resolidification as well as the action of a shockwave when the plasma stream impacts the sample surface.

The irradiated titanium surface shows a smaller roughness in comparison with Cu and especially with Al. Therefore melt motion in this case should be more noticeable as is demonstrated in Fig. 3 showing the result for a composed target with an inner titanium disk and a copper outside ring. The inner edge of the copper ring is covered by a melted titanium film. The estimated maximum velocity of the melt motion is about 1–5 m/s. Moreover, titanium droplets are seen on the copper surface, thus again demonstrating droplet splashing.

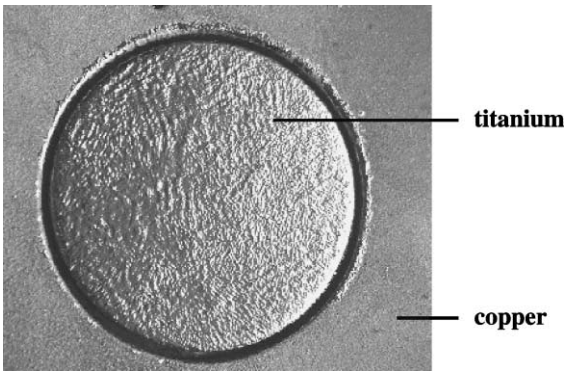

Fig. 3. Image of composite Ti–Cu sample irradiated with QSPA plasma streams.

3.2. Sample erosion

Mass losses of irradiated materials versus the number of pulses are presented in Fig. 4 for irradiations at the PPA and the QSPA facility. Under PPA plasma irradiation larger mass losses are observed during the first 5 pulses, which is possibly due to material outgassing and ejection of weakly bounded fragments. Afterwards the quantity of eroded material decreases, and the mass defect practically becomes constant. The mass losses are about 0.03, 0.06 and 0.18 mg/pulse for Ti, Cu and Al samples, accordingly. It should be noted that due to the plasma shielding effect at the QSPA high-power plasma interaction with a target [7,9], only a small part of the plasma stream energy density is delivered to the sample surface. According to the measurements of the shielding efficiency because of the rather short pulse duration and the lower density of the plasma stream generated at the PPA facility, the shielding efficiency in the PPA exposures is smaller in comparison with the shielding

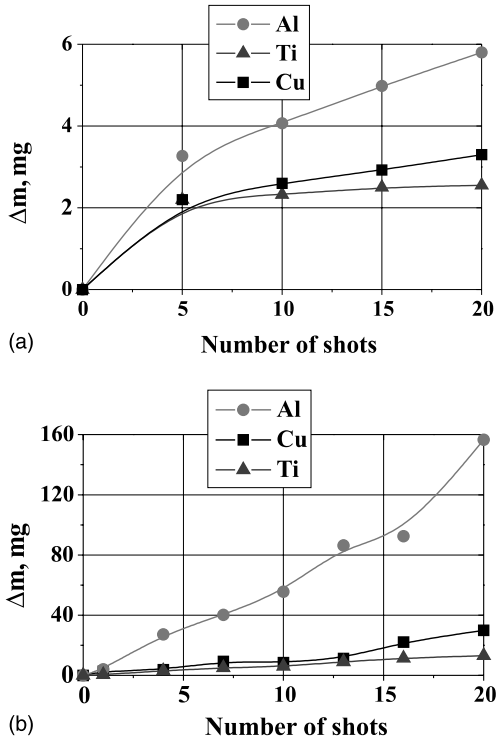

Fig. 4. Mass loss of irradiated samples as a function of the number of exposures: (a) PPA irradiation and (b) QSPA irradiation.

efficiency in the QSPA exposures [7]. In the PPA exposures the deposited energy density typically achieves 65% of the incoming plasma stream energy density.

Under QSPA exposure no decrease of the mass loss was observed with increasing number of pulses. Due to the higher value of the mass losses the effect of the surface cleaning practically remains without influence. Moreover, the deviation from the linear dependence (especially for Al and Cu) is due to the mass loss caused by melt motion toward the sample edge. Only an average mass loss can be estimated for QSPA irradiation. The minimum mass loss was observed for Ti – 0.65 mg/pulse, the maximum one – for aluminum 7.5 mg/pulse.

3.3. Cross-sectional analysis

The analysis of cross-sections of the copper samples has shown an extremely irregular microstructure in the resolidified melt layer. The layer thickness is not uniform and fluctuates between 30 and 90 μm. The average distance between maximums of melt layer thickness is about 100–140 μm. The size and the shape of the copper crystal grains in the melt layer and in the sample volume practically do not change (Fig. 5(a)). At larger magnification fine cracks of wavy form, parallel to the irradiated surface are observed in the resolidified melt layer. The cracks in the resolidified layer indicate microstresses and confirm the results of X-ray analysis described above.

For the aluminum sample the melt layer thickness varied within 30–150 μm. The microstructure in the resolidified layer consists of elongated crystalline grains of wavy form (Fig. 5(b)). In some parts of the melt layer pores were observed. A rather irregular melt layer with triangular cavities was observed for titanium samples. The layer thickness varies from 20 to 100 μm. Besides the initial phase the melt layer involves martensite-like needles of rather small size confirming polyamorphous transformations in the resolidified Ti layer. The thickness of the melt layer in steel samples was also non-uniform and typically achieved 60 μm in QSPA exposures. For PPA irradiation the cross-sectional analysis shows the resolidified layer with more uniform thickness. Variations of the melt layer thickness were observed only for Al samples.

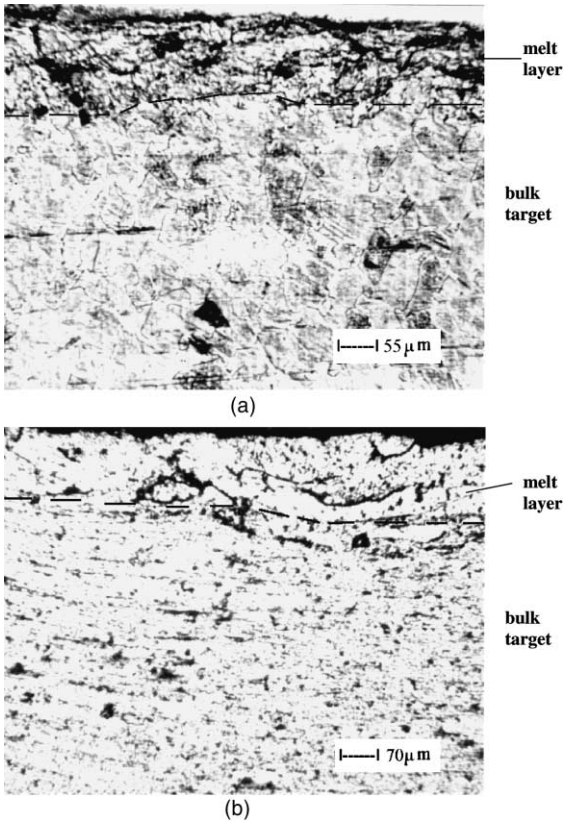

Fig. 5. Cross-sections of samples irradiated at the QSPA facility: (a) copper and (b) aluminum.

4. Conclusions

From the exposure experiments with high power plasma streams using different materials the following conclusions can be drawn: as a result of intense heating, a melt layer appears at the surface of the metal targets. The non-uniform (in thickness) resolidified melt layer shows a complicated structure with a considerable surface roughness, which can amount up to several hundreds of microns after 15 pulses of irradiation (several millimeters for aluminum). Increasing the heat load results in an increase of the intensity of droplet splashing with redeposition of the splashed material in the neighborhood of the melted area. The considerable surface roughness is due to onset of boiling, bubble expansion and bubble collapse, to the onset of melt motion and the formation of a Kelvin–Helmholtz instability. The surface roughness increases with increasing deposited energy value and duration of the heat load.

Under the conditions realized in the QSPA experiments melt motion clearly was observed for titanium and aluminum. However melt layer erosion is masked by boiling, bubble expansion and bubble collapse and by the Kelvin–Helmholtz instability. Fine cracks and pores might play a special role in erosion, resulting in the appearance of spalling and flaking and in a change of the local heat conductivity value. As a result of pulsed heating the compressing stress leads to plastic deformation of the resolidified layers.

Acknowledgement

This work has been performed within the frame of the WTZ project UKR005-98.

References

[1] H. Wuerz, S. Pestchanyi, B. Bazylev, et al., J. Nucl. Mater. 290–293 (2001) 1138.
[2] K. Fujimura, M. Ogawa, M. Seki, Fus. Eng. Des. 19 (1992) 183.
[3] M. Ogawa, M. Araki, M. Seki, et al., Fus. Eng. Des. 19 (1992) 193.
[4] H. Wuerz et al., these Proceedings.
[5] B. Bazylev, H. Wuerz, these Proceedings.
[6] I.E. Garkusha, O.V. Byrka, V.V. Chebotarev, et al., Vacuum 58 (2000) 195.
[7] V.V. Chebotarev, I.E. Garkusha, V.V. Garkusha, et al., J. Nucl. Mater. 233–237 (1996) 736.
[8] V.V. Chebotarev, I.E. Garkusha, G.P. Glazunov, et al. 23rd EPS Conference on Controlled Fusion and Plasma Physics, Vol. II, Kiev, Ukraine, 24–28 June 1996, p. 839.
[9] H. Wuerz et al., J. Nucl. Mater. 220–222 (1995) 1066.